

Chest CT Severity Score: An Imaging Tool for Assessing Severe COVID-19

Ran Yang*^{1,2}

Xiang Li*^{1,2}

Huan Liu³

Yanling Zhen⁴

Xianxiang Zhang^{1,2}

Qiuxia Xiong^{1,2}

Yong Luo^{1,2}

Cailiang Gao^{1,2}

Wenbing Zeng^{1,2}

¹Department of Radiology, Chongqing University Three Gorges Hospital, Chongqing 404000, China.

²Department of Radiology, Chongqing Three Gorges Central Hospital, Chongqing 404000, China

³GE Healthcare, Shanghai, 201203 China

⁴Department of Radiology, Affiliated Hospital of North Sichuan Medical College, Sichuan 637000, China

* Co-first author, these two authors contributed equally to the article.

Corresponding author: Wenbing Zeng, MS

Department of Radiology, Chongqing Three Gorges Central Hospital

Chongqing 404000, China (Email: zeng_wenbing@163.com)

Project No. 2020CDJYGRH-YJ03 supported by the Fundamental Research Funds for the Central Universities.

Conflicts of interest: Authors had nothing to disclose.

Article type: Original Research

Key Results

- The dominant distribution of COVID-19 pneumonia is bilateral and posterior.
- The proposed pulmonary inflammation load score was higher in patients with severe COVID-19 in comparison with patient with mild disease.
- The optimal inflammation load score threshold for identifying severe patients was 19.5, with 83.3% sensitivity and 94% specificity.

Summary statement

The chest CT severity score could be used to rapidly identify patients with severe forms of COVID-19.

Background: Quantitative and semi-quantitative indicators to evaluate the severity of lung inflammation in Coronavirus Disease 2019 (COVID-19) could provide an objective approach to rapidly identify patients in need of hospital admission.

Purpose: To evaluate the value of chest computed tomography severity score (CT-SS) in differentiating clinical forms of COVID-19.

Materials and Methods: Inclusion of 102 patients with COVID-19 confirmed by positive real-time reverse transcriptase polymerase chain reaction on throat swabs underwent chest CT (53 men and 49 women, 15-79 years old, 84 cases with mild and 18 cases with severe disease). The CT-SS was defined by summing up individual scores from 20 lung regions; scores of 0, 1, and 2 were respectively assigned for each region if parenchymal opacification involved 0%, less than 50%, or equal or more than 50% of each region (theoretical range of CT-SS from 0 to 40). The clinical and laboratory data were collected, and patients were clinically subdivided according to disease severity by the Chinese National Health Commission guidelines.

Results: The posterior segment of upper lobe (left, 68/102; right, 68/102), superior segment of lower lobe (left, 79/102; right, 79/102), lateral basal segment (left, 79/102; right, 70/102) and posterior basal segment of lower lobe (left, 81/102; right, 83/102) were the most frequently involved sites in COVID-19. Lung opacification mainly involved the lower lobes, in comparison with middle-upper lobes. No significant differences in distribution of the disease were seen between right and left lungs. The individual scores of in each lung, as well as the total CT-SS were higher in severe COVID-19 when compared with mild cases ($P < 0.05$). The optimal CT-SS threshold for identifying severe COVID-19 was 19.5 (area under curve, 0.892), with 83.3% sensitivity and 94% specificity.

Conclusion: CT-SS could be used to quickly and objectively evaluate the severity of pulmonary involvement in COVID-19 patients.

Introduction

Since December 2019, a cluster of cases with unknown pneumonia with similar clinical manifestations suggesting viral pneumonia appeared in Wuhan City, Hubei Province, China. A new type of coronavirus was isolated from the lower respiratory tract samples, named Severe Acute Respiratory Syndrome Coronavirus-2 (SARS-CoV-2) by the International Virus Classification Commission [1]. The disease it causes was named Coronavirus Disease 2019 (COVID-19) by WHO in February 11, 2020 [2]. SARS-CoV-2 belong to β -coronavirus, which is a typical RNA virus. It is generally round or oval shaped, with a diameter of 60 to 140 nm under the electron microscope. Its outer membrane had unique spikes, about 9 to 12 nm, similar to the solar corona [3]. The study found that the SARS-CoV-2 shares 92% homology with the bat coronavirus sequence RaTG3, which suggests a zoonotic origin for this outbreak [4]. SARS-CoV-2 can spread from person-to-person [5] and has been declared a pandemic disease. The common clinical symptoms of patients with COVID-19 are fever, cough, dyspnea and fatigue, which are similar to those of severe acute respiratory syndrome coronavirus (SARS-CoV) and Middle East respiratory syndrome coronavirus (MERS-CoV) [6,7]. Severe cases can lead to acute respiratory distress syndrome, or even death. According to the severity of the patient's condition, the treatment is different. Mild patients receive antiviral, symptomatic support and oxygen therapy. However, severe cases need to be admitted to intensive care unit as soon as possible.

At present, the diagnosis of COVID-19 depends on real-time reverse transcriptase polymerase chain reaction (RT RT-PCT) or next-generation sequencing [8]. On imaging, computed tomography (CT) manifestations resemble those seen in viral pneumonias [9], with multifocal ground-glass opacities and consolidation in a peripheral distribution being the most common findings [10,11]. Although these findings lack specificity for COVID-19 diagnosis on imaging grounds, we hypothesize that CT could be used to provide objective

assessment about the extension of the lung opacities, which could be used as an imaging surrogate for disease burden. The main purpose of our study was to evaluate the performance and inter-reader concordance of a semi-quantitative CT severity score designed to identify severity of COVID-19. If feasible, such approach could expedite the identification and management of severe patients in specific instances where a fast triage method is needed.

Materials and Methods

Patients and Groups

The study was approved by the Ethics Committee of Chongqing Three Gorges Central Hospital. We retrospectively studied the patients who were diagnosed with COVID-19 from January 21, 2020 to February 5, 2020 in our hospital. According to our hospital protocol, all patients with suspected COVID-19 routinely underwent non-contrast CT examinations and were admitted in hospital for isolation and observation. CT was chosen over chest radiographs based on the assumption that the former is more sensitive to detect lung opacities.

A total of 102 patients with COVID-19 were confirmed by RT RT-PCR throat swab [12]. Patients with lung malignancy, a history of lobectomy, tuberculosis, or atelectasis were excluded from this study. According to the "Diagnosis and Treatment Program of Pneumonia of New Coronavirus Infection (Trial Fifth Edition)" [13] recommended by China's National Health Commission on February 5, 2020, COVID-19 patients are classified as having *minimal*, *common*, *severe* and *critical*. *Minimal disease* patients have subtle clinical symptoms and no lung opacities on chest imaging and have been excluded from further analyses in this study. *Common* cases have symptoms such as fever and respiratory tract, and chest imaging showing lung opacities. *Severe* cases should meet any of the following criteria: (1) respiratory distress, $RR \geq 30$ beats / min; (2) resting blood oxygen saturation $\leq 93\%$; or

(3) partial pressure of arterial blood oxygen (PaO₂) / oxygen concentration (FiO₂) ≤ 300 mmHg. *Critical* patients need to meet one of the following conditions: (1) respiratory failure and need mechanical ventilation; (2) shock; (3) other organ failure needing ICU monitoring treatment.

For the purposes of this study, *common* cases were included in the **Mild Disease** group, while *severe* and *critical* cases were merged into the **Severe Disease** group, because of the small number of cases in the latter category (n = 3).

Chest CT Severity Score Assessment

We developed a chest CT severity score (CT-SS) for assessing COVID-19 burden on the initial scan obtained at admission. This score uses lung opacification as a surrogate for extension of the disease in the lungs. The CT-SS is an adaptation of a method previously used to describe ground-glass opacity, interstitial opacity, and air trapping, which was correlated with clinical and laboratory parameters in patients after SARS [14]. According to the anatomical structure, the 18 segments of both lungs were divided into 20 regions, in which the posterior apical segment of the left upper lobe was subdivided into apical and posterior segmental regions, while the anteromedial basal segment of the left lower lobe was subdivided into anterior and basal segmental regions. The lung opacities in all of the 20 lung regions were subjectively evaluated on chest CT using a system attributing scores of 0, 1, and 2 if parenchymal opacification involved 0%, less than 50%, or equal or more than 50% of each region. The CT-SS was defined as the sum of the individual scored in the 20 lung segment regions, which may range from 0 to 40 points.

All CT images were independently reviewed by two chest radiologists with more than 10 years of experience, blinded to the clinical data and laboratory indicators, in a standard clinical Picture Archiving and Diagnostic System workstation. All thin-section CT scans

were reviewed at a window width and level of 1000 to 2000 HU and -700 to -500 HU, respectively, for lung parenchyma.

Chest CT Scan

Chest CT imaging was performed on a 16-detector CT scanner (Emotion; SIEMENS). All patients were examined in supine position. CT images were then acquired during a single inspiratory breath-hold. The scanning range was from the apex of lung to costophrenic angle. CT scan parameters: X-ray tube parameters - 120KVp, 350mAs; rotation time - 0.5 second; pitch - 1.0; section thickness – 5 mm; intersection space – 5 mm; additional reconstruction with sharp convolution kernel and a slice thickness of 1.5 mm.

Statistical Analysis

Statistical analysis was performed using R (version 3.5.1). $P < 0.05$ was regarded to demonstrate statistical significance. Quantitative data were expressed as mean \pm standard deviation or median and interquartile range. The Weighted Kappa coefficient was used to compare the consistency of two observers in each lung segment. Interrater reliability was evaluated using intraclass correlation coefficient (ICCs) for continuous variables (ICCs was classified as follows: no agreement, 0-0.2; weak agreement, 0.21-0.4; moderate agreement, 0.41-0.60; good agreement, 0.61-0.80; and excellent agreement, 0.81-1.0). All measurements were assessed with normality tests. A Chi square or Fisher exact test was used to compare the scores of each lung segment between the mild and severe groups. A Wilcoxon rank sum test was used to compare the difference of left lung, right lung and total score between the mild group and the severe group, and the Wilcoxon matched-pairs signed-rank test was used to compare the difference of scores between lower lung and middle-upper lung, left lung and right lung. Receiver operator characteristic (ROC) curve analysis was performed to calculate

the threshold, specificity, sensitivity and accuracy for discriminating the **Mild** from the **Severe** COVID-19 group.

Results

Clinical and laboratory findings

Table 1 shows the demographic and clinical data of 102 patients at the time of admission. A total of 102 patients were included in this study 84 in the **Mild** group and 18 in the **Severe** group, with respective average ages of 43.70 and 52.83 ($P = 0.004$) and male/female ratios of 43/41 and 10/8. The average body temperature of the patients was 37.5 °C (**Mild** group) and 37.8 °C (**Severe** group), and no statistical difference was found ($P= 0.464$). The most common clinical symptoms were cough (72/102, 70.59%) and fever (86/102, 84.31%). The time from onset of symptoms and respiratory rate in the **Severe** group were higher than that of the **Mild** group, while the blood oxygen saturation was decreased in the former group ($P< 0.05$). Only three patients in the **Severe** group needed mechanical ventilation, while none in the **Mild** group needed ventilatory support. The percentage and absolute lymphocyte counts were lower in the **Severe** group ($P<0.001$). The percentage of neutrophils and serum concentrations of hypersensitive C-reactive protein (HSCRP) and procalcitonin (PCT) were higher in **Severe** group in comparison with the **Mild** group ($P<0.001$).

Imaging Findings

The inter-reader ICCs for CT-SS was excellent ($n=102$, $ICC_{median}=0.925$, $ICC_{mean}=0.936$).

The scores provided by one of the two readers was randomly chosen for further analyses.

Figure 1 displays the total number of patients with lung opacities in each of the lung segments. Overall, the posterior segment of the upper lobes (left, 68/102 [66.7%]; right, 68/102 [66.7%]), the superior segment of the lower lobes (left, 79/102 [77.5%]; right, 79/102

[77.5%]), the lateral basal segments of the lower lobes (left, 79/102 [77.5%]; right, 70/102 [68.6%]), and the posterior basal segments of the lower lobes (left, 81/102 [79.4%]; right, 83/102 [81.4%]) are the most frequently involved sites in COVID-19. There were significant differences between the **Mild** and **Severe** groups lung opacity scoring in each lung region, $P < 0.05$ (**Table 2**). The left lung score was 6.0 (3.0, 8.0), right lung score was 6.0 (3.45, 8.0) and total CT-SS was 13.0 (6.0, 16.0) in the **Mild** group, while the left lung score was 12.0 (9.0, 14.0), right lung score was 12.0 (9.0, 16.05), and total CT-SS was 23.5 (20.95, 30.05) in the **Severe** group (**Table 2**, **Figure 2** and **Figure 3**). The lower lobe scores were higher than the middle-upper lobe scores in each group. However, there were no significant differences between left and right lung scores (**Table 3**). Pleural effusions were found in 7 cases and lymphadenopathy in 2 cases in the **Severe** group, while pleural effusion and lymphadenopathy were not found in the **Mild** group (**Table 4**).

ROC Curve for CT-SS

The ROC curve analysis for CT-SS is shown in **Figure 4**. The area under the ROC curve for discriminating patients in the **Mild** and **Severe** group was 0.892 (standard error, 0.05; 95% CI, 0.814-0.944), and the optimal CT-SS threshold for identifying severe patients was 19.5, with 83.3% sensitivity and 94% specificity. The number of patients with CT-SS equal to or greater than 19.5 was 15 in the **Severe** group and 5 in the **Mild**, while the number of patients with CT-SS less than 19.5 was 3 and 79, respectively, resulting in a positive predictive value (PPV) of 75.0% and a negative predictive value (NPV) for severe disease of 96.3%.

Discussion

On January 30th, 2020, the World Health Organization declared COVID-19 as the sixth public health emergency deserving international attention. COVID-19 is highly contagious

and has spread worldwide. Strategies for disease containment and patient management heavily rely on disease diagnosis [3,15,16]. However, COVID-19 testing has been challenged by limited laboratory facilities and inadequate supply of nucleic acid kits [17]. Moreover, the lack of early abnormalities on chest radiographs can lead to a large number of false negatives [18]. Thin-section chest CT is more sensitive than chest radiography, showing abnormal changes in the lung parenchyma in early stages of disease [19,20]. For these reasons, chest CT has become a forefront diagnostic method during the outbreak of COVID-19 in China [18].

The typical imaging manifestations of early COVID-19 are patchy, rounded, segmental or subsegmental ground-glass opacities, with or without consolidation [20]. Lesions are multiple and asymmetrically distributed and are more common in the peripheral areas [11,21,22]. Some imaging findings of COVID-19 overlap with those of other RNA viral infection, such as respiratory syncytial virus (RSV) and human parainfluenza virus (HPIV) [9,23]. Song et al [24] retrospectively analysed the chest CT images of 51 patients with COVID-19; the results showed that 82% of the patients had posterior lung involvement, which are closely matched with our observations. Noticeably, the dominant posterior distribution is similar to reports on SARS-CoV and MERS-CoV infection [25,26]. In our study, we also found a slight predominance of opacities in the lower lobes when compared with the middle and upper lobes, without significant differences between the right and left lung, which was also consistent with previous analyses [27].

In this study, we devised a semi-quantitative scoring method using the amount of lung opacification involving 20 lung regions as a surrogate for COVID-19 burden. We found that the CT-SS was higher in severe when compared to mild cases. Most importantly, we determined that a CT-SS threshold of 19.5 could identify severe COVID-19, with a sensitivity of 83.3% and a specificity of 94%, resulting in an NPV of 96.3%. Moreover, inter-

reader agreement was excellent between our two radiologists. We envision that this relatively straightforward method could provide objective means to expedite the identification of patients with severe disease, especially in situations of limited availability of healthcare resources.

This retrospective study has several limitations. First, the CT-SS assumes that the amount of lung opacification is a surrogate for COVID-19 burden; however, there was no histologic confirmation of the findings. Second, we chose to analyze the first chest CT obtained on admission; therefore, the studies were not controlled by the number of days since the start of symptoms, which could have potential implications for interpretation of the CT-SS. Indeed, our data shows that patients in the **Severe** group had a larger interval between beginning of symptoms and hospital admission in comparison with patients in the **Mild** group. Third, the CT-SS was only investigated within a small group ($n = 2$) of relatively experienced radiologists. Further research is needed to identify the degree of consistency of CT-SS among readers with different levels of experience. Last, external validation studies with larger cohorts in multiple centers are still necessary to determine the validity of CT-SS and the proposed threshold before clinical translation.

In conclusion, this study provides a straightforward semi-quantitative method for assessing severity of COVID-19 in the initial chest CT. A CT-SS score less than 19.5 could rule out severe or critical forms of disease with a high NPV of 96.3% in our cohort. CT-SS could be potentially used to expedite triage of patients in need of hospital admission. We envision that such approach could have value in scenarios combining high patient volumes and limited healthcare resources or PCR testing capabilities.

Acknowledgments: The authors thank Xinghua Liu, Yun Wen, Jingxian Xiong, Department of Radiology, Chongqing Three Gorges Central Hospital, for assisting with CT imaging data collection, and Xu Wang, GE Healthcare, for assisting with data statistical analysis.

References

1. Gorbalenya AE, Baker SC, Baric RS, et al. Severe acute respiratory syndrome-related coronavirus: The species and its viruses – a statement of the Coronavirus Study Group. <https://doi.org/10.1101/2020.02.07.937862> doi: bioRxiv preprint
2. WHO. Novel coronavirus – China. Feb 11, 2020. https://www.who.int/docs/default-source/coronaviruse/situation-reports/20200211-sitrep-22-ncov.pdf?sfvrsn=fb6d49b1_2.
3. Zhu N, Zhang D, Wang W, et al. A Novel Coronavirus from Patients with Pneumonia in China, 2019. *N Engl J Med* 2020 Jan 24. doi: 10.1056/NEJMoa2001017. [Epub ahead of print]
4. Peng Zhou, Xing-Lou Yang, Xian-Guang Wang, et al. Discovery of a novel coronavirus associated with the recent pneumonia outbreak in humans and its potential bat origin. bioRxiv 2020.01.22.914952; preprint doi: <https://doi.org/10.1101/2020.01.22.914952>. [Epub ahead of print].
5. Chan JF, Yuan S, Kok KH, et al. A familial cluster of pneumonia associated with the 2019 novel coronavirus indicating person-to-person transmission a study of a family cluster. *The Lancet* 2020 Jan 24. pii: S0140-6736(20)30154-9. doi: 10.1016/S0140-6736(20)30154-9. [Epub ahead of print].
6. Lee N, Hui D, Wu A, et al. A major outbreak of severe acute respiratory syndrome in Hong Kong. *N Engl J Med* 2003; 348: 1986–1994.
7. Assiri A, Al-Tawfiq JA, Al-Rabeeh AA, et al. Epidemiological, demographic, and clinical characteristics of 47 cases of Middle East respiratory syndrome coronavirus disease from Saudi Arabia: a descriptive study. *Lancet Infect Dis* 2013; 13(9): 752–761.
8. Huang C, Wang Y, Li X, et al. Clinical features of patients infected with 2019 novel coronavirus in Wuhan, China. *Lancet* 2020 Jan 24. pii: S0140-6736(20)30183-5. doi: 10.1016/S0140-6736(20)30183-5. [Epub ahead of print]
9. Koo HJ, Lim S, Choe J, et al. Radiographic and CT Features of Viral Pneumonia. *Radiographics* 2018; 38(3):719-739.
10. Pan Y, Guan H. Imaging changes in patients with 2019-nCov. *Eur Radiol*. 2020 Feb 6. doi: 10.1007/s00330-020-06713-z. [Epub ahead of print]
11. Lei J, Li J, Li X, et al. CT Imaging of the 2019 Novel Coronavirus (2019-nCoV) Pneumonia. *Radiology*. 2020 Jan 31:200236. doi: 10.1148/radiol.2020200236. [Epub ahead of print]
12. Corman VM, Landt O, Kaiser M, et al. Detection of 2019 novel coronavirus (2019-nCoV) by real-time RT-PCR. *Euro Surveill* 2020 Jan;25(3). doi: 10.2807/1560-7917.ES.2020.25.3.2000045.

13. General Office of National Health Commission. the Diagnosis and Treatment of Pneumonia Infected by Novel Coronavirus (5th Trial Edition).
http://www.gov.cn/zhengce/zhengceku/2020-02/05/content_5474791.htm
14. Chang YC, Yu CJ, Chang SC, et al. Pulmonary sequelae in convalescent patients after severe acute respiratory syndrome: evaluation with thin-section CT. *Radiology* 2005; 236(3):1067-1075.
15. Li Q, Guan X, Wu P, et al. Early Transmission Dynamics in Wuhan, China, of Novel Coronavirus–Infected Pneumonia. *N Engl J Med* 2020 Jan 29. doi: 10.1056/NEJMoa2001316. [Epub ahead of print]
16. Carlos WG, Dela Cruz CS, Cao B, et al. Novel Wuhan (2019-nCoV) Coronavirus. *Am J Respir Crit Care Med* 2020 Feb 15; 201(4): 7-8.
17. Xiao SY, Wu Y, Liu H. Evolving status of the 2019 novel coronavirus Infection: proposal of conventional serologic assays for disease diagnosis and infection monitoring [Commentary/Review]. *J Med Virol.* 2020 Feb 7. doi: 10.1002/jmv.25702. [Epub ahead of print]
18. Chinese Society of Radiology. Radiological Diagnosis of New Coronavirus Infected Pneumonitis: Expert Recommendation from the Chinese Society of Radiology (First edition). *Chin J Radiol* 2020, 54(00): E001-E001. DOI: 10.3760/cma.j.issn.1005-1201.2020.0001.
19. Paul NS, Roberts H, Butany J, et al. Radiologic Pattern of Disease in Patients with Severe Acute Respiratory Syndrome: The Toronto Experience1. *RadioGraphics* 2004; 24(2):553-563.
20. Ng MY, Lee EYP, Yang, J et al. Imaging Profile of the COVID-19 Infection: Radiologic Findings and Literature Review. *Radiol Cardiothoracic Imaging* 2020;2(1):e200034.
21. Liu P, Tan XZ. 2019 Novel Coronavirus (2019-nCoV) Pneumonia. *Radiology* 2020 Feb 04:200257. doi:10.1148/radiol.2020200257
22. Chung M, Bernheim A, Mei X, et al. CT Imaging Features of 2019 Novel Coronavirus (2019-nCoV). *Radiology* 2020 Feb 4:200230. doi: 10.1148/radiol.2020200230. [Epub ahead of print]
23. Franquet T. Imaging of Pulmonary Viral Pneumonia. *Radiology* 2011; 260(1):18-39.
24. Song F, Shi N, Shan F, et al. Emerging Coronavirus 2019-nCoV Pneumonia. *Radiology.* 2020 Feb 6:200274. doi: 10.1148/radiol.2020200274. [Epub ahead of print]
25. Wong KT, Antonio GE, Hui DS, et al. Severe acute respiratory syndrome: radiographic appearances and pattern of progression in 138 patients. *Radiology* 2003 Aug; 228(2):401-406.

26. Ajlan AM, Ahyad RA, Jamjoom LG, et al. Middle East respiratory syndrome coronavirus (MERS-CoV) infection: chest CT findings. *AJR Am J Roentgenol* 2014 Oct; 203(4):782-787.
27. Wu J, Wu X, Zeng W, et al. Chest CT Findings in Patients with Corona Virus Disease 2019 and its Relationship with Clinical Features. *Invest Radiol* 2020 Feb 21. doi: 10.1097/RLI.0000000000000670.

Table 1. Demographic and Clinical Data of 102 Patients with COVID-19 pneumonia

Variable	Mild (n=84)	Severe (n=18)	Statistics	P-value
Sex				
Male	43 (51.19%)	10 (55.56%)	0.113	0.737
Female	41 (48.81%)	8 (44.44%)		
Age				
Mean±SD	43.70±11.71	52.83±12.96	-2.946	0.004*
Range	15-78	31-79		
Cough				
No	27 (32.14 %)	3 (16.67 %)	1.71	0.191
Yes	57 (67.86 %)	15 (83.33 %)		
Expectoration				
No	79 (94.05 %)	15 (83.33 %)	1.105	0.293
Yes	5 (5.95 %)	3 (16.67 %)		
Fever				
No	13 (15.48 %)	3 (16.67 %)	0.053	0.817
Yes	71 (84.52 %)	15 (83.33 %)		
Temperature	37.50 (36.90, 38.00)	37.80 (37.29, 38.00)	-0.733	0.464
Mechanical Ventilation				
No	84 (100.00%)	15 (83.33%)	inf	0.005*
Yes	0 (0.00%)	3 (16.67%)		
Time of Onset (days)	6.00 (4.00, 9.00)	9.00 (7.00, 12.05)	-2.971	0.003*
RR (beats/min; 12–20)	20.00 (19.00, 20.00)	25.00 (20.00, 33.25)	-4.736	<0.001*
SO ₂ (≥0.95)	0.97 (0.96, 0.98)	0.92 (0.88, 0.93)	6.276	<0.001*
WBC (10 ⁹ /L; 3.5–9.5)	5.00 (4.00, 6.30)	5.20 (3.50, 6.53)	0.075	0.941
NEU% (0.45–0.75)	0.66±0.11	0.79±0.10	-4.422	<0.001*
LYM% (0.20–0.50)	0.25 (0.19, 0.31)	0.15 (0.09, 0.22)	4.17	<0.001*
NEU (10 ⁹ /L; 1.8–6.3)	3.40 (2.42, 4.17)	3.35 (2.45, 5.25)	-0.584	0.559
LYM (10 ⁹ /L; 1.1–3.2)	1.21 (0.90, 1.50)	0.68 (0.46, 0.96)	4.45	<0.001*
HSCRP (mg/L; 0–11)	11.29 (2.71, 37.46)	107.91 (47.41, 135.93)	-5.267	<0.001*
PCT (ng/ml; <0.046)	0.04 (0.03, 0.07)	0.09 (0.06, 0.21)	-4.499	<0.001*

* *P* values less than 0.05 were considered statistically significant.

Notes. —WBC: white blood cell, NEU: neutrophils, LYM: lymphocytes, HSCRP:

hypersensitive C-reactive protein, PCT: Procalcitonin, SO₂: Blood Oxygen Saturation, RR:

Respiratory Rate.

Table 2. Comparison of scores of each lung segment between the two groups

Variable	Sample	Mild (n=84)	Severe (n=18)	<i>P</i>	<i>Kappa</i>
anterior segment (L)					
0	59	53 (63.10%)	6 (33.33%)	0.002	0.648
1	41	31 (36.90%)	10 (55.56%)		
2	2	0 (0.00%)	2 (11.11%)		
apical segment (L)					
0	56	52 (61.90%)	4 (22.22%)	<0.001	0.776
1	44	32 (38.10%)	12 (66.67%)		
2	2	0 (0.00%)	2 (11.11%)		
posterior segment (L)					
0	34	32 (38.10%)	2 (11.11%)	<0.001	0.782
1	54	46 (54.76%)	8 (44.44%)		
2	14	6 (7.14%)	8 (44.44%)		
superior lingular segment (L)					
0	30	29 (34.52%)	1 (5.56%)	0.002	0.829
1	65	52 (61.90%)	13 (72.22%)		
2	7	3 (3.57%)	4 (22.22%)		
inferior lingular segment (L)					
0	39	38 (45.24%)	1 (5.56%)	<0.001	0.798
1	51	42 (50.00%)	9 (50.00%)		
2	12	4 (4.76%)	8 (44.44%)		
superior segment (L)					
0	23	22 (26.19%)	1 (5.56%)	<0.001	0.883
1	56	51 (60.71%)	5 (27.78%)		
2	23	11 (13.10%)	12 (66.67%)		
anterior basal segment (L)					
0	59	55 (65.48%)	4 (22.22%)	<0.001	0.687
1	37	29 (34.52%)	8 (44.44%)		
2	6	0 (0.00%)	6 (33.33%)		
medial basal segment (L)					
0	76	69 (82.14%)	7 (38.89%)	<0.001	0.799
1	21	15 (17.86%)	6 (33.33%)		
2	5	0 (0.00%)	5 (27.78%)		
lateral basal segment (L)					
0	23	23 (27.38%)	0 (0.00%)	<0.001	0.816
1	68	58 (69.05%)	10 (55.56%)		
2	11	3 (3.57%)	8 (44.44%)		
posterior basal segment (L)					
0	21	21 (25.00%)	0 (0.00%)	<0.001	0.807
1	64	55 (65.48%)	9 (50.00%)		
2	17	8 (9.52%)	9 (50.00%)		
anterior segment (R)					
0	38	36 (42.86%)	2 (11.11%)	0.006	0.757
1	61	47 (55.95%)	14 (77.78%)		
2	3	1 (1.19%)	2 (11.11%)		
apical segment (R)					

0	60	54 (64.29%)	6 (33.33%)	0.011	0.721
1	39	29 (34.52%)	10 (55.56%)		
2	3	1 (1.19%)	2 (11.11%)		
posterior segment (R)					
0	34	31 (36.90%)	3 (16.67%)	<0.001	0.878
1	59	51 (60.71%)	8 (44.44%)		
2	9	2 (2.38%)	7 (38.89%)		
medial segment (R)					
0	54	50 (59.52%)	4 (22.22%)	<0.001	0.891
1	42	34 (40.48%)	8 (44.44%)		
2	6	0 (0.00%)	6 (33.33%)		
lateral segment (R)					
0	35	33 (39.29%)	2 (11.11%)	<0.001	0.966
1	56	47 (55.95%)	9 (50.00%)		
2	11	4 (4.76%)	7 (38.89%)		
superior segment (R)					
0	23	21 (25.00%)	2 (11.11%)	<0.001	0.858
1	63	58 (69.05%)	5 (27.78%)		
2	16	5 (5.95%)	11 (61.11%)		
anterior basal segment (R)					
0	53	49 (58.33%)	4 (22.22%)	<0.001	0.770
1	43	35 (41.67%)	8 (44.44%)		
2	6	0 (0.00%)	6 (33.33%)		
medial basal segment (R)					
0	59	55 (65.48%)	4 (22.22%)	<0.001	0.793
1	37	28 (33.33%)	9 (50.00%)		
2	6	1 (1.19%)	5 (27.78%)		
lateral basal segment (R)					
0	32	30 (35.71%)	2 (11.11%)	<0.001	0.664
1	58	50 (59.52%)	8 (44.44%)		
2	12	4 (4.76%)	8 (44.44%)		
posterior basal segment (R)					
0	19	18 (21.43%)	1 (5.56%)	0.001	0.761
1	61	54 (64.29%)	7 (38.89%)		
2	22	12 (14.29%)	10 (55.56%)		
Score of left lung	102	6.00 (3.00, 8.00)	12.00 (9.00, 14.00)	<0.001	0.925 [#]
Score of right lung	102	6.00 (3.45, 8.00)	12.00 (9.00, 16.05)	<0.001	0.892 [#]
Total score	102	13.00 (6.00, 16.00)	23.50 (20.95, 30.05)	<0.001	0.990 [#]

[#] ICC: intraclass correlation coefficient.

Notes. L: left lung, R: right lung.

Table 3. Comparison of left lung score and right lung score, lower lung score and upper-middle lung score

Variable	Left lung	Right lung	<i>P</i>	Middle-upper lung	Lower lung	<i>P</i>
Mild (n=84)	6.0 (3.0, 8.0)	6.0 (3.45, 8.0)	0.583	6.0 (2.75,9.0)	7.0 (4.0,8.0)	0.011*
Severe (n=18)	12.0 (9.0, 14.0)	12.0 (9.0, 16.05)	0.938	11.0 (10.0,13.5)	12.5 (9.25,16.5)	0.038*

* *P* values less than 0.05 were considered statistically significant.

Note: Data were presented as median (IQR). Wilcoxon matched-pairs signed-rank test was used.

Table 4. Secondary CT Findings of 102 Patients with COVID-19

Variable	Mild (n=84)	Severe (n=18)	Total	<i>P</i>
Pleural Effusions	0	7	7	0.833
Lymphadenopathy	0	2	2	
Total	0	9	9	

Note.—Fisher’s exact test was used.

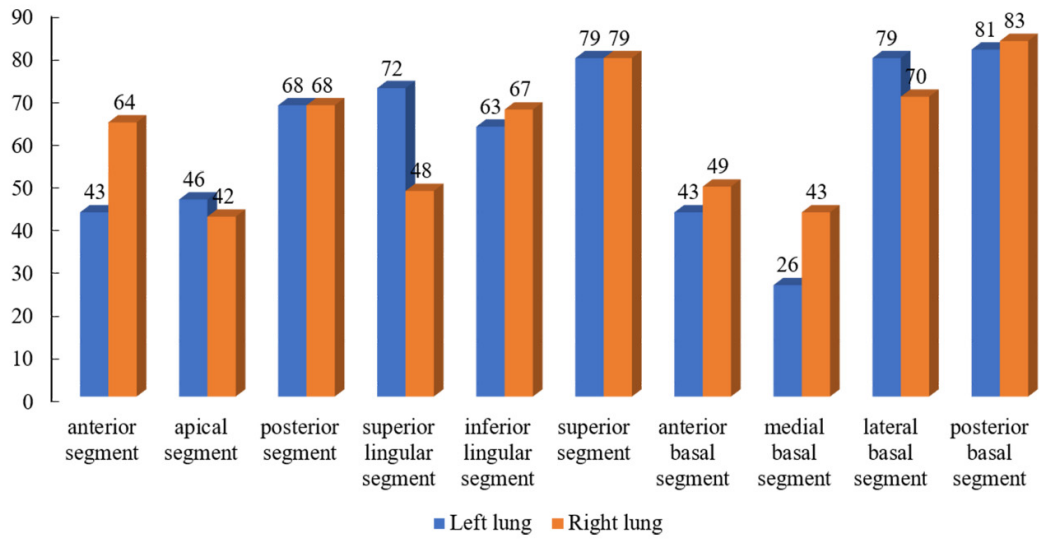


Figure 1. Number of patients involved in each lung segment.

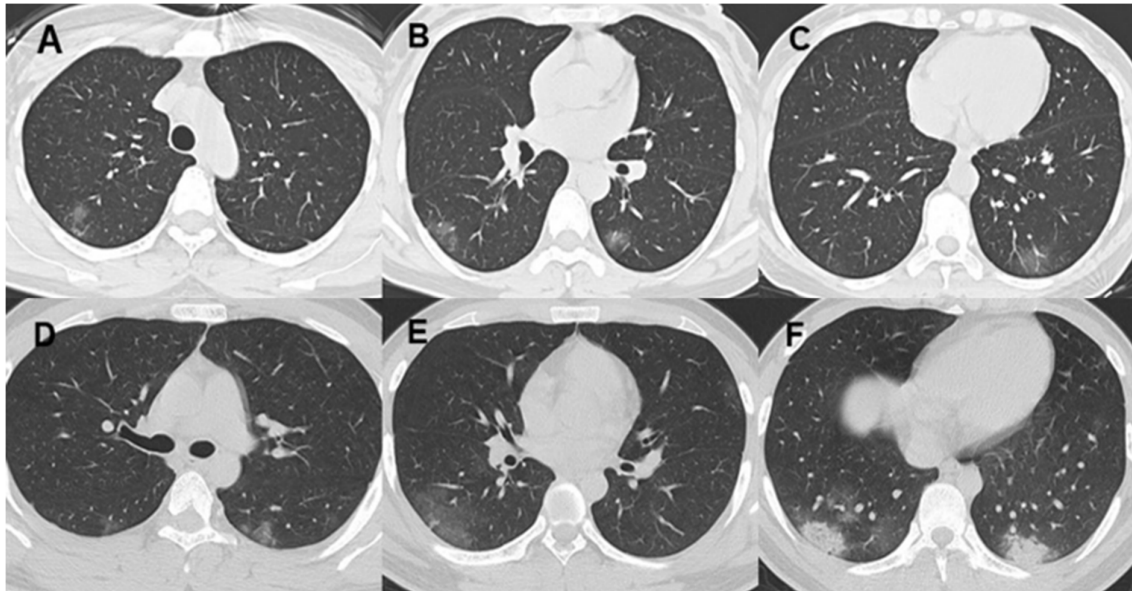


Figure 2. A-C. Non-contrast chest CT images of a 46 year old woman with mild COVID-19 pneumonia. CT scans show ground-glass opacities in the posterior segment of right upper lobe, superior segment of bilateral lungs and posterior basal segment of right left lobe, the

CT-SS is 4. D-F. Non-contrast chest CT images of a 20 year old man with mild COVID-19 pneumonia. CT scans show ground-glass opacities and consolidation in multiple lung segments, the CT-SS is 7.

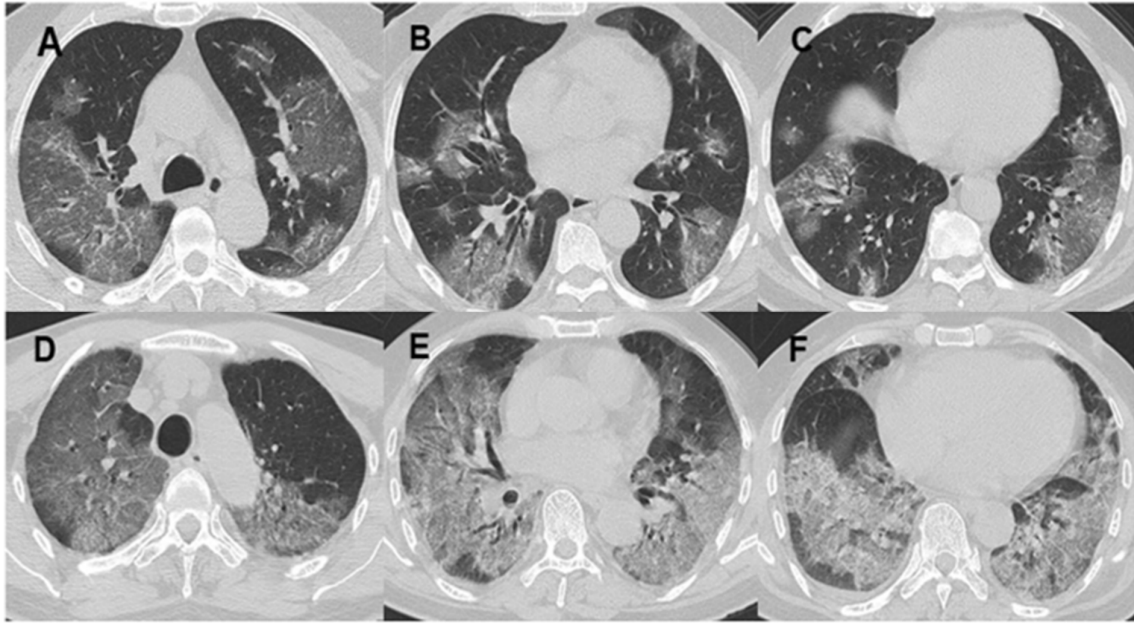


Figure 3. A-C. Non-contrast chest CT images of a 56 year old man with severe COVID-19 pneumonia. CT scans show multiple ground-glass opacities in multiple lung segments, the CT-SS is 28. D-F. Non-contrast chest CT images of a 69 year old man with severe COVID-19 pneumonia. CT scans show multiple ground-glass opacities and septal thickening, the imaging manifestation is the so-called “white lungs”, the CT-SS is 35.

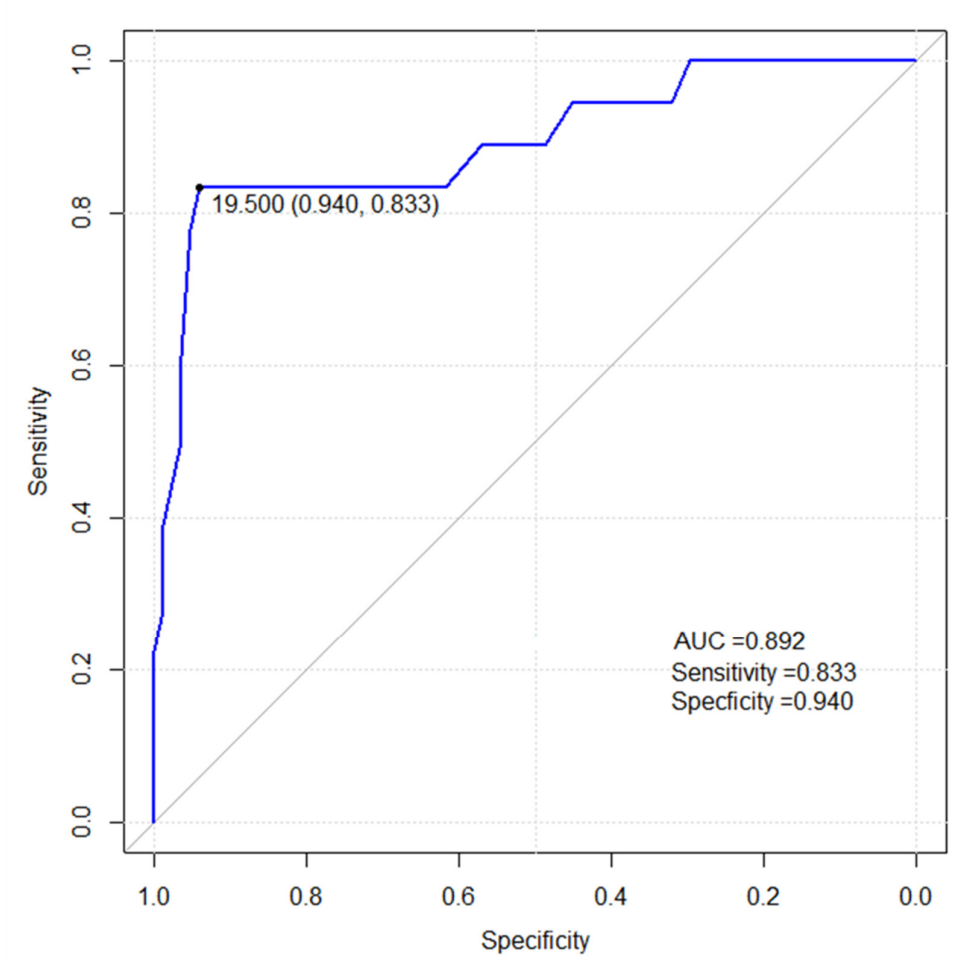


Figure 4. ROC Curve for CT-SS.